International Journal of Heat and Mass Transfer xxx (2009) xxx–xxx

Contents lists available at ScienceDirect

International Journal of Heat and Mass Transfer

journal homepage: www.elsevier.com/locate/ijhmt

Improved flow pattern map for accurate prediction of the heat transfer coefficients during condensation of R-134a in smooth horizontal tubes and within the low-mass flux range

R. Suliman, L. Liebenberg, J.P. Meyer *

Department of Mechanical and Aeronautical Engineering, University of Pretoria, Pretoria 0002, South Africa

ARTICLE INFO

Article history:
Received 4 April 2008
Received in revised form 29 August 2009
Accepted 29 August 2009
Available online xxxx

Keywords:
Condensation
Smooth tube
Flow pattern
Heat transfer
Refrigerant

ABSTRACT

This paper presents an improved flow pattern map for predicting the heat transfer coefficients during condensation of R-134a inside a smooth horizontal tube. Experimental tests were conducted over the low-mass flux range of 75–300 kg/m^2 s, at a nominal saturation temperature of 40 °C, and with the test section vapour qualities ranging from 0.76 down to 0.03. This represents points within the annular, intermittent and stratified flow regimes. The results were used to modify the Thome–El Hajal flow pattern map to include a transition region between the stratified-wavy and annular or intermittent flow regimes. The revised flow pattern-based heat transfer correlation predicted the experimental data to a mean deviation of less than 6%.

1. Introduction

In-tube condensation of refrigerants in water- and air-cooled condensers is extensively used in the air-conditioning, refrigeration, automotive and process industries. Accurate and unified methods are required to optimally design these systems [1]. Higher energy efficiency requirements, material and space saving considerations, economic incentives and the move to more environmentally–friendly refrigerants have further emphasised this need.

During flow condensation inside horizontal tubes, the two-phase flow may be controlled by vapour shear or gravity forces. The stratified and stratified-wavy flow regimes are dominated by gravitational forces, while vapour shear forces are the controlling forces in the annular flow regime. Since the heat and momentum transfer processes are strongly influenced by the local flow regime, and particularly on the relative importance of inertial and gravitational forces on the liquid film, any accurate prediction of the two-phase heat transfer should be based on the analysis of the prevailing flow pattern.

Analogous to predicting the transition from laminar to turbulent flow in single-phase flow, numerous flow pattern maps have been developed for predicting two-phase flow regime transitions under adiabatic and diabatic conditions [2,3]. Specifically for condensation, the first flow pattern maps were proposed by Breber et al. [4] and later Tandon et al. [5]. Kattan et al. [6–9] proposed the first comprehensive flow-boiling model for evaporation inside horizontal tubes based on the local flow pattern and a newly developed diabatic flow pattern map.

This new approach resulted in significant improvements in the accuracy and reliability of heat transfer predictions compared with previous methods. As a consequence, several new condensation heat transfer models based on local flow patterns have been proposed by, among others, Shao and Granryd [10] and Cavallini et al. [11]. El Hajal et al. [12] adapted the flow-boiling two-phase flow pattern map, originally developed by Kattan et al., for condensation inside horizontal tubes. Due to the high reduced pressures during condensation and because of the sensitivity of flow pattern transitions, heat transfer coefficients and pressure drop to void fraction, El Hajal et al. [12] and Collier and Thome [13] proposed a new log-mean method for predicting void fractions for pressures ranging from atmospheric up to near the critical pressure.

The Thome–El Hajal flow pattern map [12] is a modification of the Steiner [14] map, which in turn is a modification of the original Taitel and Dukler [15] map. El Hajal et al. [12] simplified the implementation of the map by bringing the Rouhani and Axelsson [16] void fraction equation into the method to eliminate its iterative solution scheme. Also, the changes proposed by Zürcher et al. [17] were implemented to ensure better prediction of the transition curves from annular to stratified-wavy flow, and from stratified-wavy to stratified flow.

* Corresponding author. Tel.: +27 (0) 12 420 3104; fax: +27 (0) 12 362 5124.
E-mail address: jmeyer@up.ac.za (J.P. Meyer).

0017-9310/$ - see front matter © 2009 Elsevier Ltd. All rights reserved.
doi:10.1016/j.ijheatmasstransfer.2009.08.017

Nomenclature

A	area (m^2)
d	diameter (m)
EB	energy balance
Fr	Froude number
G	mass flux (kg/m^2 s)
g	gravitational acceleration (m/s^2)
h	enthalpy (J/kg)
k	thermal conductivity (W/m K)
L	length of test section (m)
$\dot{m}$	mass flow (kg/s)
$\dot{Q}$	heat transferred (W)
R_w	wall thermal resistance (K/W)
T	temperature (°C)
We	Weber number
x	vapour quality
z	axial distance along test section axis (m)

Greek symbols

α	heat transfer coefficient (W/m^2 K)
θ	stratification angle (rad)
ρ	density (kg/m^3)

Subscripts

b	bulk
Cu	copper
c	convective
d	dimensionless
f	film
H_2O	water
i	inner
IA	intermittent–annular transition
in	inlet
l	liquid
o	outer
pre	pre-condenser
ref	refrigerant
s	surface
sat	saturation
$strat$	stratified
$test$	test section
$trans$	transition
v	vapour
w	wall
$wavy$	wavy transition

For flow condensation, saturated vapour enters a condenser tube and forms either a thin liquid film around the perimeter of the tube as an annular flow or a liquid layer in the bottom of the tube and a gravity-controlled condensing film around the upper perimeter as a stratified or stratified-wavy flow [12,18]. At very high mass fluxes, it is also possible that the flow goes into mist flow, in which liquid droplets are entrained in a largely gaseous flow. This, however, rarely happens, and has not been studied much, due to the low number of processes which encounter condensation at such high mass fluxes [19].

Several condensation heat transfer models have been proposed over the years. However, each correlation is given with suitable validity ranges of parameters within which it can be used for calculating the heat transfer coefficient. Very few models are general and cover the entire range of two-phase regimes. Furthermore, no accurate analytical model exists and, therefore, it is necessary to experiment and develop empirical correlations for practical use. The recent models of Cavallini et al. [20] and Thome et al. [18] cover all flow regimes. The model of Thome et al. [18] is capable of predicting heat transfer coefficients to within ±25%. However, the lines depicting transitions between flow regimes could occur over a mass flux range of about 50 kg/m^2 s [18]. The aim of this work was to improve the accuracy of the Thome et al. [18] flow pattern-based heat transfer model based on experiments within the low-mass flux range, particularly the transition between stratified-wavy and annular or intermittent flow.

2. Experimental facility

The experimental facility (Fig. 1) consisted of two main sub-systems: the vapour-compression cycle and the water cycles. The vapour-compression cycle consisted of a hermetically sealed scroll compressor with a nominal cooling capacity of 10 kW. The condenser line split into two lines, the test line and the bypass line. Each line had its own electronic expansion valve (EEV). The test line EEV was used to control the mass flow through the test line, and the bypass EEV was used to control the test pressure. The test line comprised of four water-cooled condensers, namely a pre-condenser to control the inlet vapour quality, a straight horizontal tube-in-tube counterflow test heat exchanger, with water in the annulus and refrigerant on the inside, and two extra heat exchangers, namely the post-condenser and the sub-cooler. The post-condenser was used to control the refrigerant state in the post-condenser, which must be saturated liquid at the exit. The bypass line had one large water-cooled heat exchanger. After the expansion valves, the lines combined and entered a water-heated evaporator, followed by a suction-accumulator.

The test line was constructed of a 9.53 mm (3/8 in.) outer diameter copper tube with an inner diameter of 8.38 mm. At the entrance of the test line, a straight calming section, 50-tube diameters long, was utilised to ensure fully developed flow [21]. Cylindrical sight glasses were positioned at the inlet and exit of the test section to act as insulators against axial conduction and also to allow for high-speed visual images of the flow to be taken, using a high-speed camera. The outer-wall temperatures of the inner tube along the 1.546 m test section were measured at seven stations using four T-type thermocouples per station, which were placed around the tube perimeter. These thermocouples were soldered to the outer-wall of the inner tube. The inlet and outlet temperatures of the inner tube were measured before the inlet and after the outlet sight glasses. All of the thermocouples used in this experimental system were calibrated against a high-precision Pt-100 resistance temperature detector. The refrigerant mass flow was measured using a Coriolis mass flow meter. Another section (50 diameters long) was installed at the exit to ensure that the flow in the test section and exit sight glass was not disturbed.

The oil concentration in the refrigerant was measured using the ASHRAE Standard [22], and was determined as 1.8% on average.

The water cycle consisted of a hot and a cold side. The water was used to exchange heat with the refrigerant side at the condensers (cold water) and the evaporator (hot water). Each heat exchanger's water supply rate was controlled using electronically actuated three-way valves, while the required pressure head was supplied by centrifugal pumps.

The water was stored in two insulated 5000-l tanks. These two tanks shared a 70 kW heating/50 kW cooling dual function heat pump and were thermostatically-controlled between 13–17 and 23–27 °C, respectively. If any of the two tanks were at the set tem-

Please cite this article in press as: R. Suliman et al., Improved flow pattern map for accurate prediction of the heat transfer coefficients during condensation of R-134a in smooth horizontal tubes and within the low-mass flux range, Int. J. Heat Mass Transfer (2009), doi:10.1016/j.ijheatmasstransfer.2009.08.017

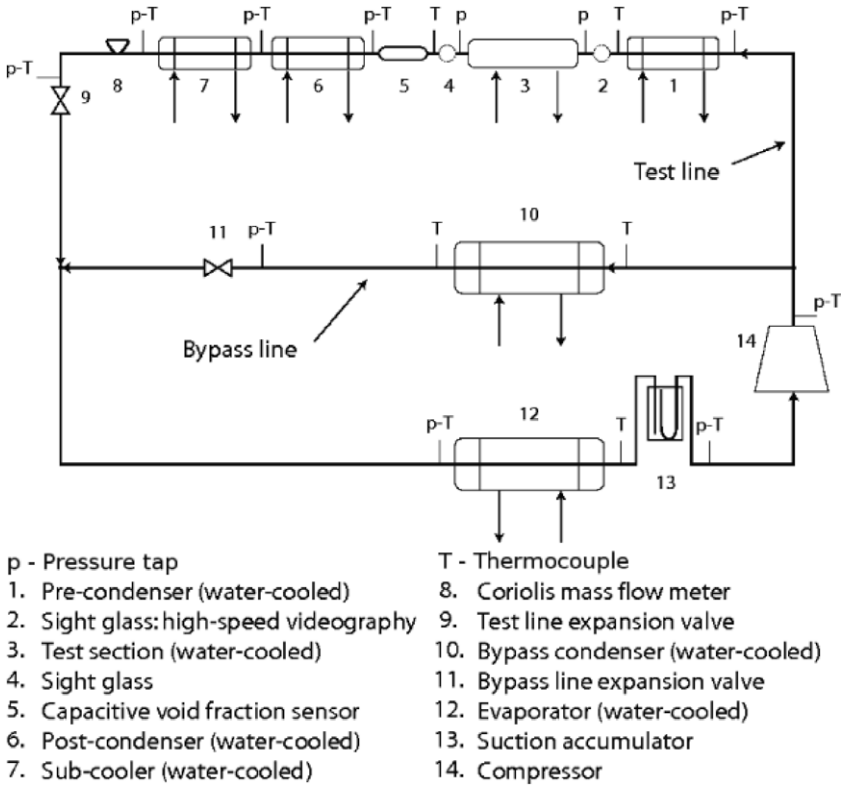

Fig. 1. Schematic diagram of the experimental layout.

perature, the heat exchanger for that side was switched to an air-cooled radiator. The size of the tanks and the size of the heat pump allowed the experimental set-up to run indefinitely.

The water flow rates through the pre-, test- and post-condensers were measured using separate Coriolis flow meters, while the ancillary heat exchangers' water mass flow rates were measured using vane-type flow meters. The inlet and outlet test-line heat exchangers' temperatures were measured using T-type thermocouples, also calibrated against a Pt-100 resistance temperature device.

Steady-state conditions were assumed when the energy balance error of the test section was less than 1%, and the temperatures and pressures of the system were constant for a period of at least 10 min. Further, experimental conditions were also maintained such that the vapour quality difference over the test section was less than 10%, although most were less than 5%.

The experimental uncertainties of the instruments are given in Table 1 and were calculated using the method described by Kline and McCintock [23].

3. Data reduction

The properties of the refrigerant at the inlet of the pre-condenser and outlet of the post-condenser were determined by temperature and pressure measurements. From these measurements, the thermo-physical properties of the condensing refrigerant were determined by utilising data from a refrigerant property database [24] and from XProps [25].

Table 1
Experimental uncertainties.

Measurement	Uncertainty
Refrigerant temperature	0.11 °C
Refrigerant mass flow	0.1%
Inlet vapour quality	3.2%
Vapour quality drop	5%
Heat transfer coefficient	4.9%

The vapour quality at the inlet of the test section was calculated from the enthalpies as

$$x_{in} = \frac{h_{in,test} - h_l}{h_v - h_l} \tag{1}$$

The enthalpies h_v and h_l were evaluated at the saturation temperature and pressure measured at the inlet of the test section. The enthalpy at the inlet of the test section, $h_{in,test}$, lay within the two-phase region and was obtained from the enthalpy at the inlet of the pre-condenser, the water-side heat transferred and the refrigerant mass flow rate:

$$h_{in,test} = h_{in,pre} - \left| \frac{\dot{Q}_{pre,H_2O}}{\dot{m}_{ref}} \right| \tag{2}$$

The enthalpy at the inlet of the pre-condenser, $h_{in,pre}$, could be inferred from the temperature and pressure at the pre-condenser inlet since this state lay in the superheated region. The quality at the outlet of the test section was calculated in much the same way as that at the inlet, except that the outlet enthalpy was used as opposed to the inlet enthalpy.

The average vapour quality of the test section was determined by the arithmetic mean of the inlet and outlet vapour qualities. To generate accurate results, the mean vapour quality drop over the test section was on the order of 5% [26], with a maximum of 10%.

The heat transfer coefficient was calculated using the mean wall temperature of the test section, the heat transferred into the water side of the test section and the refrigerant bulk temperature between the inlet and outlet of the test section. Instead of using an arithmetic average to calculate the mean wall temperature, a more representative and accurate trapezoidal numerical integration method was used:

Please cite this article in press as: R. Suliman et al., Improved flow pattern map for accurate prediction of the heat transfer coefficients during condensation of R-134a in smooth horizontal tubes and within the low-mass flux range, Int. J. Heat Mass Transfer (2009), doi:10.1016/j.ijheatmasstransfer.2009.08.017

$$T_{w,o} = \frac{1}{L}\sum_{j=1}^{6}\left[\left(T_{w,o}^{j} + T_{w,o}^{j+1}\right)\left(\frac{z_{j+1} - z_j}{2}\right)\right] \quad (3)$$

where $T_{w,o}^{j}$ is the average temperature at the jth measurement location along the test section and $(z_{j+1} - z_j)$ is the distance between measurement locations.

The inner-wall temperature was then calculated as

$$T_{w,i} = T_{w,o} + |\dot{Q}_{H_2O} \cdot R_w| \quad (4)$$

where R_w is the thermal resistance of the copper inner-tube wall, given by

$$R_w = \frac{ln(d_{o,i}/d_{i,i})}{2\pi k_{Cu} L} \quad (5)$$

Finally, by re-arranging Newton's law of cooling, the experimental heat transfer coefficients could be calculated:

$$\alpha = \left|\frac{\dot{Q}_{H_2O}}{A_s(T_{w,i} - T_{b,ref})}\right| \quad (6)$$

4. Heat transfer results

Condensation tests were performed with R-134a over a mass flux ranging from 75 to 300 kg/m^2 s and with the vapour quality varying from 0.03 to 0.76. A total of 74 data points were obtained in this range. This test matrix is shown overlaid on the Thome–El Hajal flow pattern map [12] in Fig. 2. The test matrix covers a wide proportion of the low-mass flux range and includes data within the annular, intermittent and stratified flow regimes.

Each data point was an average of 400 samples taken over a continuous period of 4–5 min under steady-state conditions, making each data point a fairly accurate representation. The mean testing point information for the data points is summarised in Table 2.

The oil concentration in the refrigerant was measured using the ASHRAE Standard 41.4 [22]. The results showed that the oil concentration was negligible at low vapour qualities, due to the relatively low speed of liquid, and was on average 1.8% at the higher vapour qualities, i.e. at vapour qualities greater than 0.45. Shao and Granryd [27] studied the effect of oil entrainment with R-134a and concluded that a 2% oil concentration results in a 10% heat transfer degradation and a 5% oil concentration results in 20% heat transfer degradation. Other studies undertaken by Schlager et al. [28], Sur and Azer [29] and Eckels and Pate [30] all report a similar conclusion; a degradation in the heat transfer due to the presence of the lubricant. To correct for this oil concentration the experimental heat transfer coefficients for which the oil concentration is not negligible, i.e. at vapour qualities greater than 0.45, was increased by 8%. This resulted in an improvement in the prediction of the heat transfer at these points. This approach is justified, based on the above-mentioned studies. It is acknowledged, however, that a more accurate approach would require inline density measurements and an update of the thermophysical properties. This was, however, not done in this study and is a point to be investigated in future studies.

Table 2
Mean testing point information.

Measurand	Mean	Standard deviation
T_{sat}	39.9 °C	±1.0 °C
EB^*	0.81%	±0.35%
G	Test-dependent	Max: ±3.35 kg/m^2 s

* $EB = \left|\frac{(\dot{Q}_{ref} - \dot{Q}_{H2O})}{(\dot{Q}_{ref} + \dot{Q}_{H2O})/2}\right| \times 100$.

The heat transfer coefficients measured are quasi-local values that represent a mean heat transfer coefficient for a small change in vapour quality from the inlet to the outlet of the test section. The main parameters which may influence the heat transfer performance in this study are the mass flux, vapour quality and driving temperature difference. Other influential parameters are the saturation temperature and reduced pressure. However, these were kept constant in this study. The importance of all these parameters is dependent on the prevailing test conditions. The

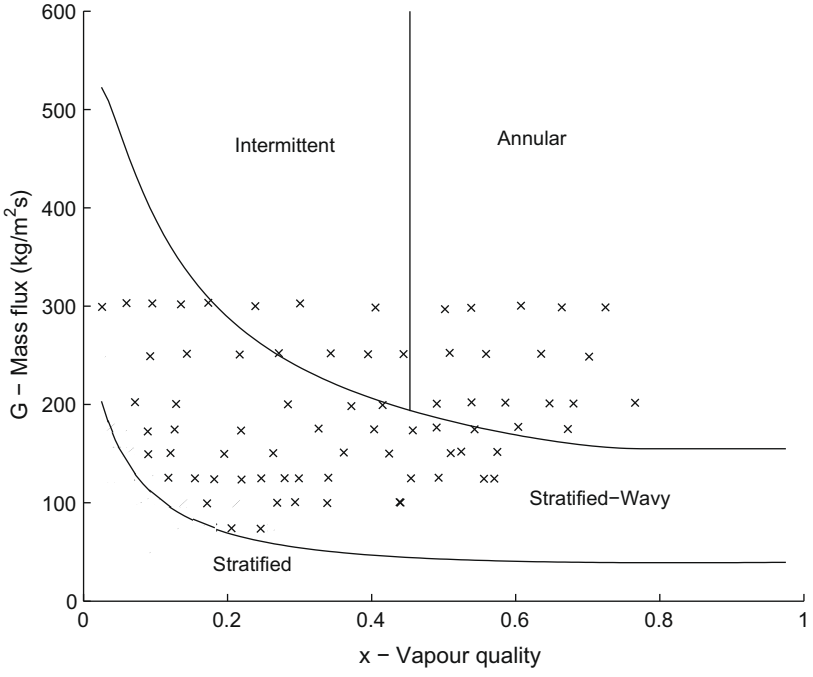

Fig. 2. Experimental test matrix overlaid on the Thome–El Hajal flow pattern map [12] for condensing R-134a in an 8.38 mm inner diameter smooth tube and at a nominal saturation temperature of 40 °C.

Please cite this article in press as: R. Suliman et al., Improved flow pattern map for accurate prediction of the heat transfer coefficients during condensation of R-134a in smooth horizontal tubes and within the low-mass flux range, Int. J. Heat Mass Transfer (2009), doi:10.1016/j.ijheatmasstransfer.2009.08.017

measured heat transfer coefficients, after correcting for oil entrainment, are analysed against these parameters below.

Fig. 3 shows the heat transfer coefficients plotted against mass flux. The figure shows the great stability achieved with mass flux during testing. The figure also shows the increase in heat transfer as mass flux is increased. At low mass fluxes, the vapour velocities are low and the flow patterns typically lie in the stratified and stratified-wavy regimes. In these flow regimes there is a thick liquid layer at the bottom of the tube which results in a high thermal resistance to heat transfer. Laminar film condensation dominates this heat transfer with a correspondingly low heat transfer coefficient. At higher mass fluxes, the vapour velocities increase and the flow takes on an intermittent or fully developed annular flow pattern. The liquid film is much thinner is this regime resulting in a lower thermal resistance. Forced convective condensation is the dominant heat transfer mechanism with correspondingly higher heat transfer coefficients.

Fig. 4 shows the heat transfer data plotted as a function of vapour quality at various mass fluxes. There is a similar trend at all the mass fluxes; the heat transfer coefficient decreases with decreasing vapour quality. This trend is expected since as condensation proceeds, the vapour quality and vapour velocity decreases.

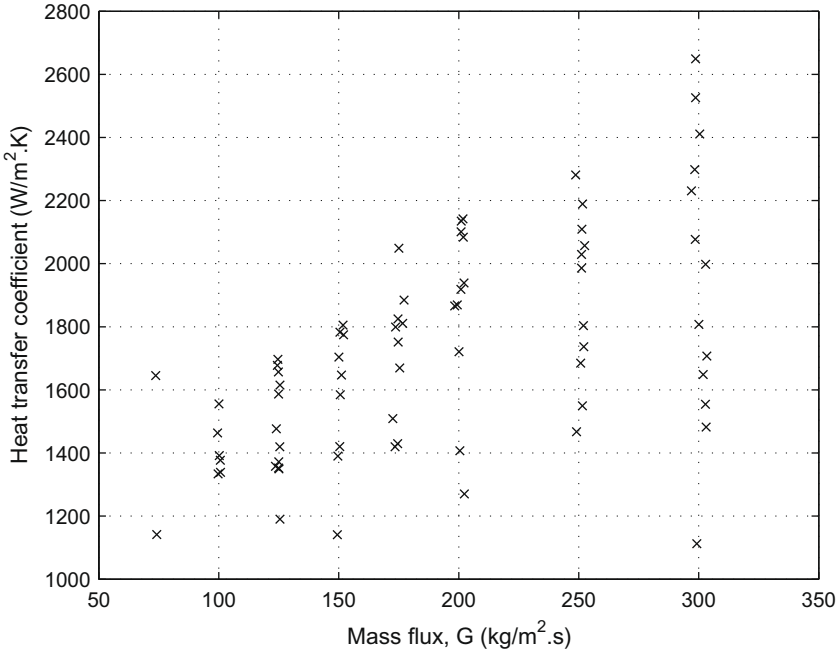

Fig. 3. Experimental heat transfer coefficients plotted against mass flux.

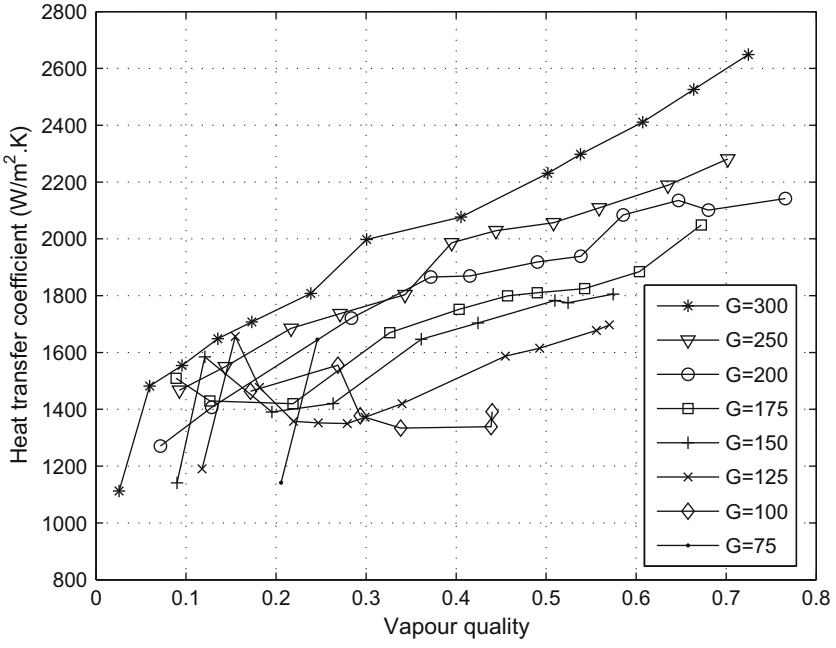

Fig. 4. Experimental heat transfer coefficients plotted against vapour quality.

Please cite this article in press as: R. Suliman et al., Improved flow pattern map for accurate prediction of the heat transfer coefficients during condensation of R-134a in smooth horizontal tubes and within the low-mass flux range, Int. J. Heat Mass Transfer (2009), doi:10.1016/j.ijheatmasstransfer.2009.08.017

This corresponds to a decrease in the vapour shear forces at the interface and a resulting lower heat transfer coefficient. This effect is most significant at high mass fluxes and high vapour qualities. This figure shows the same trend in results when compared with that previously published by other authors [18,31]. However, this trend is not as pronounced as that published by either Cavallini et al. [31] or Thome et al. [18]. This is because the mass fluxes tested in this study (up to 300 kg/m^2 s) were not high enough for the vapour shear forces to completely overcome the gravitational forces present.

A plot of the heat transfer coefficients against the product of mass flux and vapour quality, which is representative of an inertial term, is shown in Fig. 5. This figure shows that at high mass fluxes, there is a large dependence of the heat transfer coefficient on vapour quality. Vapour shear forces are significant and result in a high rate of increase of heat transfer with vapour quality. At low mass fluxes, and thus low heat transfer coefficients, there is less evident dependence on vapour quality. Vapour shear forces become negligible, compared with gravitational forces, and the flow tends towards a stratified-wavy or even fully stratified flow pattern.

There is a large influence of the temperature difference (saturation temperature minus wall temperature) on the heat transfer results as shown in Fig. 6. Heat transfer coefficient increases as

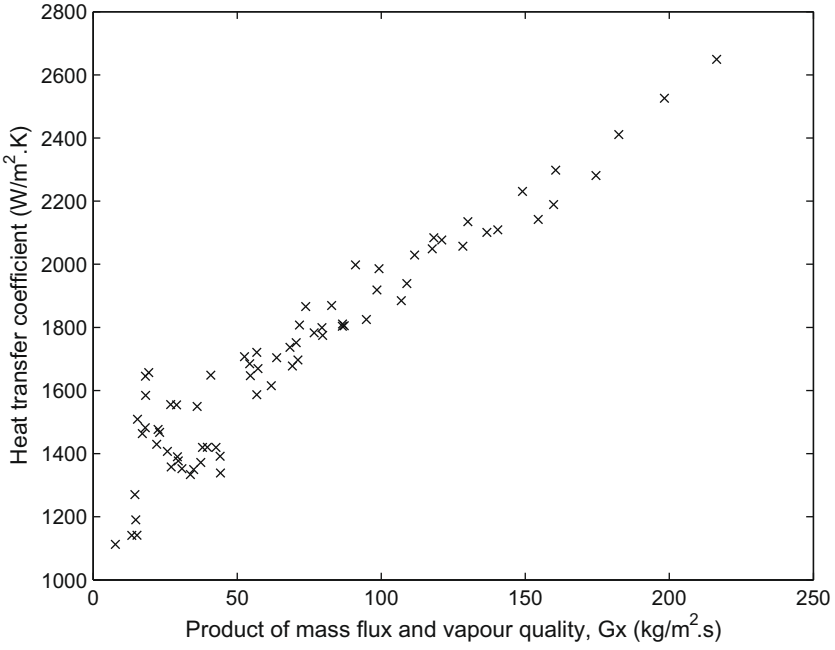

Fig. 5. Experimental heat transfer coefficients plotted against the product Gx.

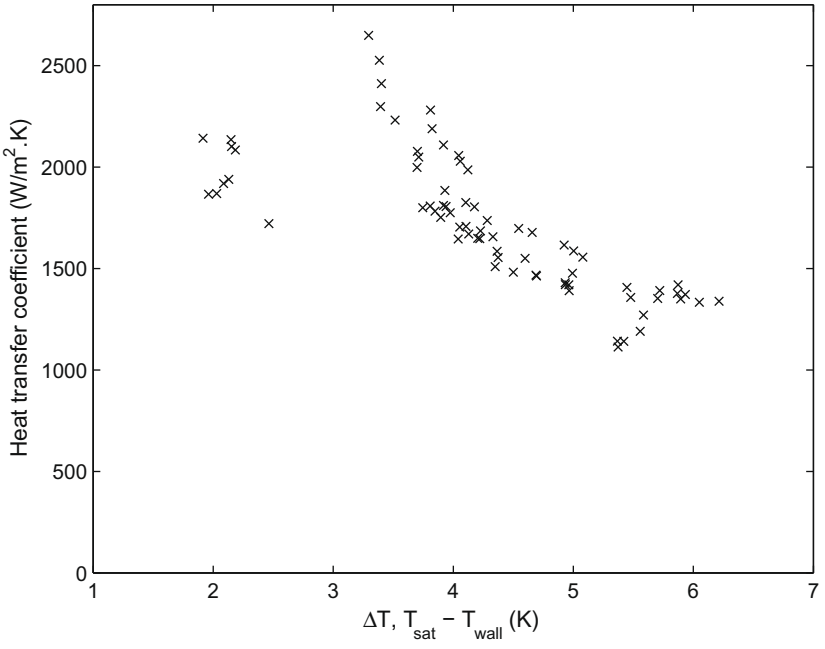

Fig. 6. Experimental heat transfer coefficients plotted against ΔT, $(T_{sat} - T_{wall})$.

Please cite this article in press as: R. Suliman et al., Improved flow pattern map for accurate prediction of the heat transfer coefficients during condensation of R-134a in smooth horizontal tubes and within the low-mass flux range, Int. J. Heat Mass Transfer (2009), doi:10.1016/j.ijheatmasstransfer.2009.08.017

the temperature difference decreases. At low mass fluxes, and thus low heat transfer coefficients, gravity is the dominant force and the temperature difference is the main driving mechanism. As the mass flux and heat transfer coefficient is increased, there is less dependence on the temperature difference. At even higher mass fluxes (not part of this study), there will be no dependence on the temperature difference and forced convection will be the major driving mechanism. The results correspond to Nusselt's falling film theory which predicts the heat transfer coefficient to be inversely proportional to the temperature difference to the power 1/4 during film condensation [32].

It is known that in the annular flow regime the heat transfer coefficient varies with mass flux, vapour quality and saturation temperature (kept constant in this study) and in the stratified-wavy and fully stratified flow regimes, the heat transfer coefficient is mainly dependent on the temperature difference [33]. The above experimental results show that the majority of the data are ΔT-dependent, thus suggesting stratified-wavy flow.

5. Comparison with leading correlations

Recent studies on condensation heat transfer have shown that the local flow regime strongly influences the heat and momentum transfer processes and any accurate prediction of the two-phase heat transfer should be based on the analysis of the prevailing flow pattern. The most recent efforts to take this into account have been made by Cavallini et al. [11] and Thome et al. [18] in two different but validated ways. Cavallini et al. [20] simplified their previous model with the aim of establishing an easy and ready-to-use model. The measured heat transfer coefficients are compared with both aforementioned models below.

The measured heat transfer coefficients are compared with the expected heat transfer coefficients, calculated as proposed by Thome [18], in Fig. 7. The results show a mean deviation of 15%. However, only 82% of the total data fell within the ±25% deviation lines. The results based on the Cavallini et al. [20] correlation show a mean deviation of 18%, as shown in Fig. 8. Similarly, only 79% of the total data fell within the ±25% deviation lines. The majority of this deviation occurred at the higher heat transfer coefficients.

6. Improved correlation

Useful information about flow patterns and the temperature dependence of the experimental data can be obtained by plotting the data on a flow pattern map, with the Martinelli parameter on the abscissa and the dimensionless gas velocity on the ordinate. This type of map was first proposed by Breber et al. [4]. The experimental test matrix is shown overlaid on this map in Fig. 9. Also shown is the transition line proposed by Cavallini et al. [20]. The results, corresponding with that from Fig. 6, show that the majority of the data are ΔT-dependent, implying stratified-wavy flow.

Further analysis of the data points that were being overpredicted by the Thome et al. [18] heat transfer correlation showed that these points lay close to the stratified-wavy to annular and intermittent transition curve. It is known that higher heat transfer coefficients are expected in the annular and intermittent flow regimes as there is only a thin liquid film around the perimeter of the tube and therefore a low thermal resistance. In the stratified-wavy and stratified flow regimes there is a thick liquid layer at the bottom of the tube which results in a high thermal resistance to heat transfer. The Thome–El Hajal flow pattern map may therefore not be predicting the flow pattern accurately.

A sensitivity analysis was done to determine which parameter had the greatest influence on the heat transfer coefficient results. This was done by perturbing the various dependent parameters in the stratified-wavy-transition-line equation. It was found that as the stratified-wavy transition line moved upwards, the points that were heavily overpredicted fell within the stratified-wavy flow regime and the heat transfer prediction was a lot closer to the measured value. Based on the significant improvement in accuracy of the heat transfer coefficient results, it could therefore be deduced that the flow pattern map was incorrectly predicting the flow pattern and that the stratified-wavy transition line needed to be moved further upwards.

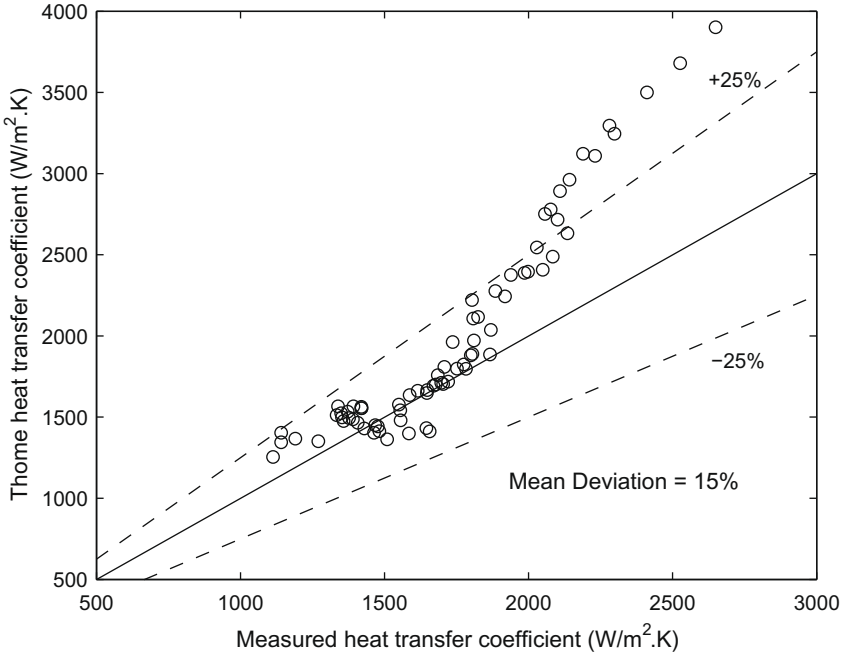

Fig. 7. Measured heat transfer coefficients compared with the Thome [18] heat transfer coefficient.

Please cite this article in press as: R. Suliman et al., Improved flow pattern map for accurate prediction of the heat transfer coefficients during condensation of R-134a in smooth horizontal tubes and within the low-mass flux range, Int. J. Heat Mass Transfer (2009), doi:10.1016/j.ijheatmasstransfer.2009.08.017

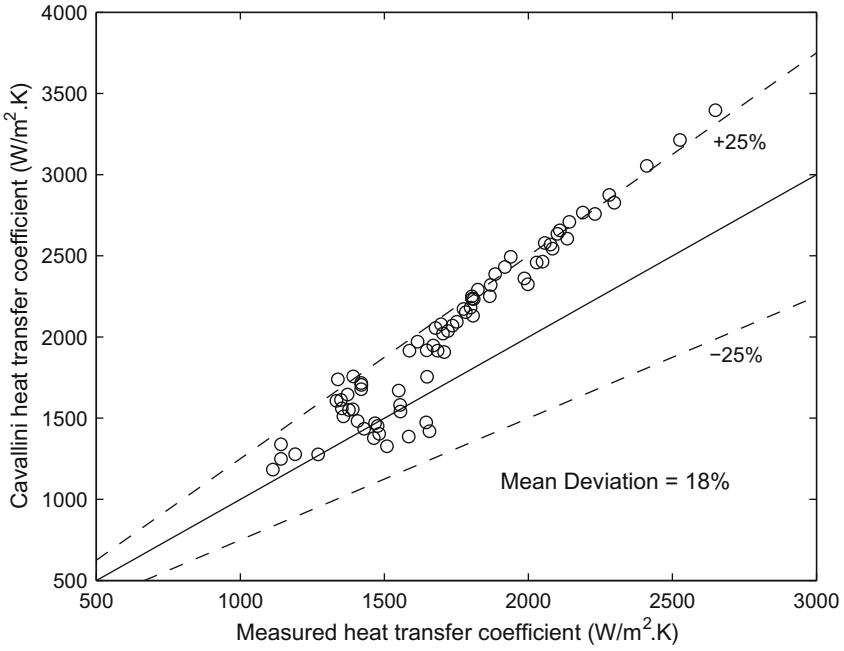

Fig. 8. Measured heat transfer coefficients compared with the Cavallini [20] heat transfer coefficient.

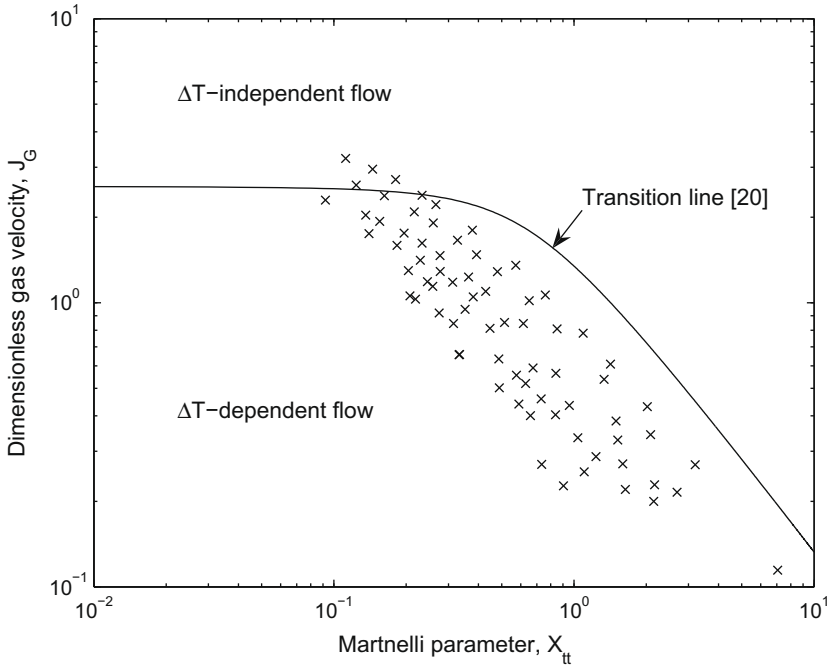

Fig. 9. Experimental test matrix overlaid on the Cavallini et al. [20] heat transfer model.

The equation describing the stratified-wavy transition line, G_{wavy}, is reproduced below for convenience [12]:

$$G_{wavy} = \left[\frac{16A_{v,d}^3 gd\rho_l\rho_v}{x^2\pi^2(1-(2h_{l,d}-1)^2)^{0.5}}\left[\frac{\pi^2}{25h_{l,d}^2}\cdot\left(\frac{We}{Fr}\right)_l^{-1.023}+1\right]\right]^{0.5} + 50 - 75^{-(x^2-0.97)^2/x(1-x)} \quad (7)$$

In the equation above, the Weber number, *We*, represents the ratio of inertial to surface tension forces. The Froude number, *Fr*, represents the ratio of inertial to gravitational forces. The ratio of Weber-to-Froude number therefore represents the ratio of gravitational to surface tension forces. It gives the relative strength of gravitational pull, i.e. how much the liquid wants to drain away, to the surface tension forces, i.e. how much the fluid wants to stick to the tube surface or the condensate retention at the top of the tube. It is known now that the points perceived to be in the annular flow regime were actually following a stratified-wavy flow pattern and so the Froude number, *Fr*, was the important number that needed to be increased to take into account the waves within the flow. The exponent of the Weber-to-Froude ratio therefore needed

Please cite this article in press as: R. Suliman et al., Improved flow pattern map for accurate prediction of the heat transfer coefficients during condensation of R-134a in smooth horizontal tubes and within the low-mass flux range, Int. J. Heat Mass Transfer (2009), doi:10.1016/j.ijheatmasstransfer.2009.08.017

to be increased. After some iteration it was found that by changing the Weber-to-Froude exponent as well as the constant term in Eq. (7), a much better estimate of the experimental measurements could be obtained. A new transition line, G_{trans}, was therefore defined and is given by Eq. (8):

$$G_{trans} = \left[\frac{16A_{v,d}^3 g d \rho_l \rho_v}{x^2\pi^2(1-(2h_{l,d}-1)^2)^{0.5}}\left[\frac{\pi^2}{25h_{l,d}^2}\cdot\left(\frac{We}{Fr}\right)_l^{-0.4}+1\right]\right]^{0.5} + 80 - 75^{-(x^2-0.97)^2/x(1-x)} \quad (8)$$

Eq. (8) therefore represents a new transition line on the Thome–El Hajal flow pattern map [12]. The region between this transition line and the stratified-wavy transition line is termed a 'transition' regime, in which a stratification angle needed to be taken into account. As in the stratified-wavy region of the Thome et al. correlation, the stratified angle was obtained by assuming a quadratic interpolation between its maximum value of θ_{strat} at G_{strat} and its minimum value of 0 at G_{trans}:

$$\theta = \theta_{strat}\left[\frac{(G_{trans}-G)}{(G_{trans}-G_{strat})}\right]^{0.5} \quad (9)$$

The local condensing heat transfer coefficient was then calculated by

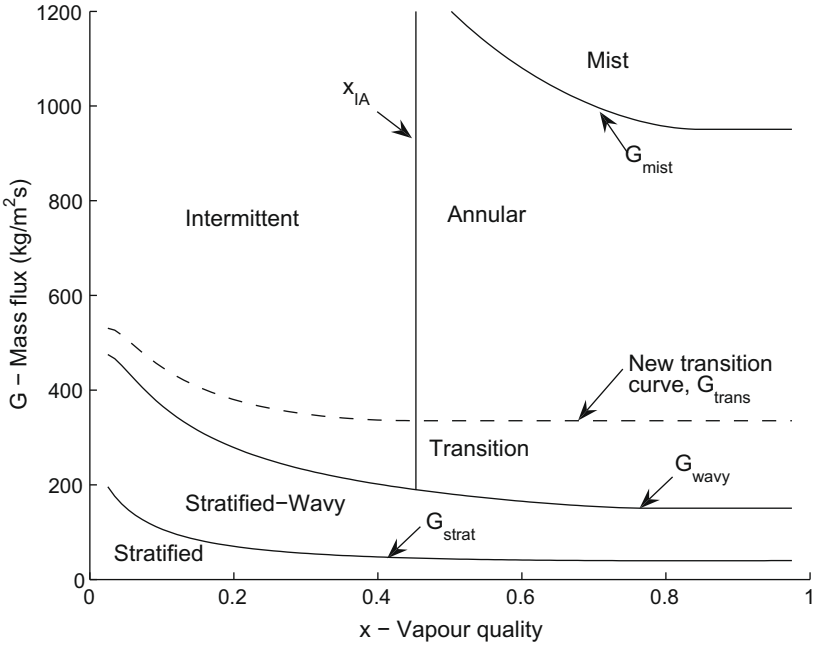

Fig. 10. Improved flow pattern map.

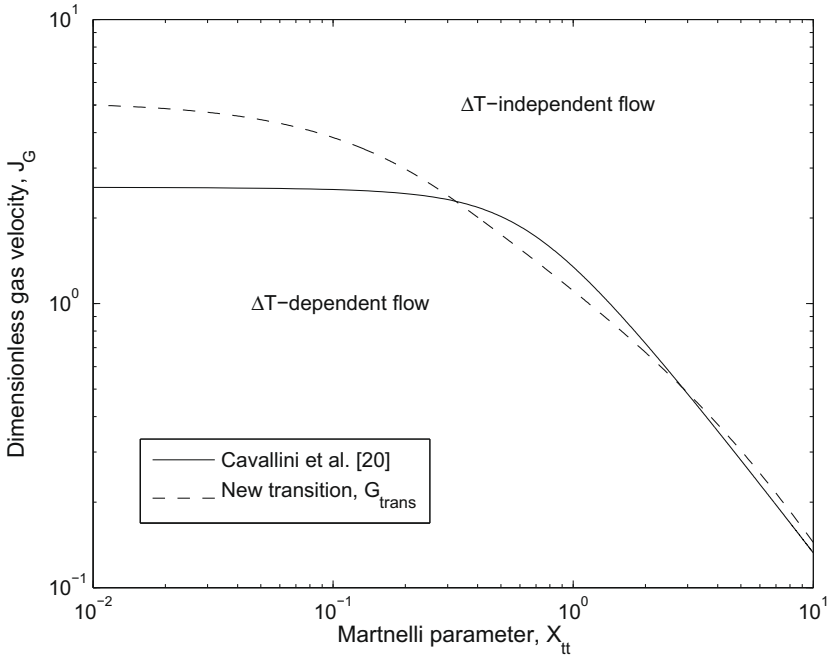

Fig. 11. Annular–intermittent to stratified-wavy transition line shown on a dimensionless gas velocity versus Martinelli parameter map.

Please cite this article in press as: R. Suliman et al., Improved flow pattern map for accurate prediction of the heat transfer coefficients during condensation of R-134a in smooth horizontal tubes and within the low-mass flux range, Int. J. Heat Mass Transfer (2009), doi:10.1016/j.ijheatmasstransfer.2009.08.017

$$\alpha = \frac{\alpha_f \theta + (2\pi - \theta)\alpha_c}{2\pi} \quad (10)$$

where α_f is the falling-film or gravitational-based coefficient and α_c is the convective or shear-stress-based coefficient as calculated from the Thome et al. [18] correlation.

This result represents an improved flow pattern-based heat transfer correlation. The revised flow pattern map with the 'transition' region developed is shown on a mass flux versus vapour quality map in Fig. 10. The annular–intermittent to stratified-wavy transition line is also shown on a dimensionless gas velocity versus Martinelli parameter map in Fig. 11.

Fig. 12 shows the results of the experimental heat transfer coefficient compared with the improved flow pattern-based heat transfer correlation. As can be seen from the figure, the experimental results compare extremely well with the new predicted values. The mean deviation has improved drastically from 15% (based on the Thome [18] correlation) to less than 6%. Furthermore, all of the data points now fall within the ±25% deviation lines, which is an improvement in accuracy.

7. Validation

The raw data (290 additional data points) from three independent heat transfer laboratories were obtained (the same datasets as described in [18]), which have determined heat transfer coefficients for R-134a, at almost the same saturation temperature, but over a wider mass flux range, and for different tube diameters. The datasets are summarised in Table 3.

The results of the experimental heat transfer coefficient compared with the Thome heat transfer correlation [18] and the improved flow pattern-based heat transfer correlation (Eqs. (8)–(10)) for the three aforementioned datasets are summarised in Table 4. In the first row, the mean percentage deviation of the experimental heat transfer coefficient with respect to the Thome et al. [18] heat transfer coefficient is shown. The mean percentage deviation with respect to the revised flow pattern-based heat transfer correlation is presented in the second row and the resulting percentage improvement is shown in the final row.

Table 3
Condensation heat transfer database.

Author(s)	Data points	Diameter (mm)	Mass flux range (kg/m^2 s)	T_{sat} (°C)
Current study	74	8.4	75–300	39–41
Cavallini et al.	49	8.0	63–756	36–42
Dobson-Chato	196	3.1 and 7.0	26–661	34–46
Shao	45	6.0	121–302	39–40

Table 4
Results of the experimental heat transfer coefficient compared with the Thome heat transfer correlation [18] and the improved flow pattern-based heat transfer correlation.

	Current study (%)	Cavallini (%)	Dobson (%)	Shao (%)
Thome et al. correlation [18]	15	11	22	26
Improved correlation (Eqs. (8)–(10))	6	11	22	14
Percentage improvement	+8.7	+0.1	−0.5	+11.5

From Table 4, it follows that the revised correlation significantly improves the data of Shao, while it does not have any major influence on the other two datasets. Furthermore, the majority of Shao's data lay within a similar region to the current study, between 120 and 300 kg/m^2 s. It can thus be concluded that the improved flow pattern-based heat transfer correlation is quite effective in the low-mass flux range and does not have any major negative influence at other conditions.

8. Conclusion

Flow condensation experiments were conducted in a smooth tube, utilising refrigerant R-134a at a nominal saturation temperature of 40 °C and over the mass flux range of 75–300 kg/m^2 s.

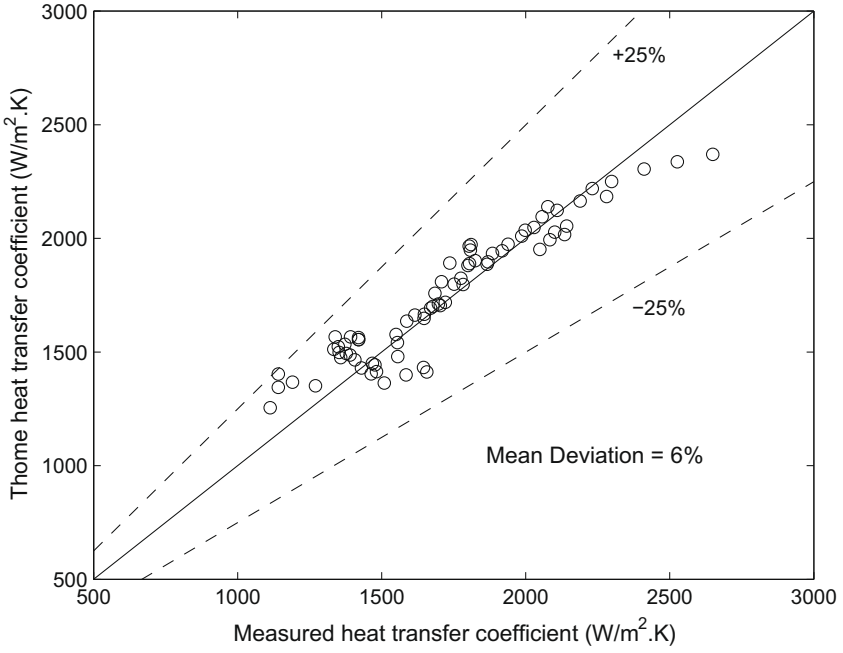

Fig. 12. Measured heat transfer coefficients compared with the revised correlation.

Please cite this article in press as: R. Suliman et al., Improved flow pattern map for accurate prediction of the heat transfer coefficients during condensation of R-134a in smooth horizontal tubes and within the low-mass flux range, Int. J. Heat Mass Transfer (2009), doi:10.1016/j.ijheatmasstransfer.2009.08.017

The experimental heat transfer coefficients, when analysed against mass flux, vapour quality and temperature difference, showed that the majority of the data are ΔT-dependent, implying stratified-wavy flow. When compared with the Thome et al. [18] correlation, the heat transfer coefficients showed a mean deviation of 15%. However, a large deviation in results occurred at the higher heat transfer coefficients, where 18% of the data points were over-predicted. Most of these datapoints were found to be in the annular and intermittent regimes.

An improved flow pattern map with a 'transition' region between stratified-wavy and annular or intermittent flows was developed. The revised correlation improved the results to a mean deviation of less than 6%, with all of the data points falling within the ±25% deviation lines. The improved correlation was also tested with data from three international heat transfer laboratories. It resulted in a significant improvement in one of the laboratories' results and it did not have any negative effect on the other results. Overall, the revised flow pattern-based heat transfer correlation improves the prediction of heat transfer within the low-mass flux range.

Acknowledgements

Mr. Marcel Christians and Mr. Eugene van Rooyen designed and built the experimental facility for their master's studies and the authors also greatly appreciate their guidance and assistance throughout this project.

Special thanks go to Professor John Thome for supplying data from other international laboratories.

References

[1] J.R. Thome, Boiling of new refrigerants: a state-of-the-art review, Int. J. Refrig. 19 (7) (1996) 435–457.
[2] L. Liebenberg, A.E. Bergles, J.P. Meyer, A review of refrigerant condensation in horizontal micro-fin tubes, in: Proceedings of the ASME Advanced Energy Systems Division, 2001, pp. 155–168.
[3] L. Liebenberg, J.P. Meyer, Refrigerant condensation flow regimes in enhanced tubes and their effect on heat transfer coefficients and pressure drops, Heat Transfer Eng. 29 (6) (2008) 506–520.
[4] G. Breber, J.W. Palen, J. Taborek, Prediction of horizontal tube-side condensation of pure components using flow regime criteria, J. Heat Transfer 102 (3) (1980) 471–476.
[5] T.N. Tandon, H.K. Varma, C.P. Gupta, A new flow regime map for condensation inside horizontal tubes, J. Heat Transfer 104 (N4) (1982) 763–768.
[6] N. Kattan, J.R. Thome, D. Favrat, Measurement and prediction of two-phase flow patterns for new refrigerants inside horizontal tubes, ASHRAE Trans. 101 (1995) 1251–1257.
[7] N. Kattan, J.R. Thome, D. Favrat, Boiling of R-134a and R-123 in a microfin tube, in: Proceedings of the 19th Int. Congr. of Refrigeration, The Hague, Netherlands, 1995, pp. 337–344.
[8] N. Kattan, J.R. Thome, D. Favrat, Flow boiling in horizontal tubes. Part 1: Development of a diabatic two-phase flow pattern map, J. Heat Transfer 120 (1) (1998) 140–147.
[9] N. Kattan, J.R. Thome, D. Favrat, Flow boiling in horizontal tubes. Part 3: Development of a new heat transfer model based on flow patterns, J. Heat Transfer 120 (1) (1998) 156–165.
[10] D.W. Shao, E. Granryd, Flow pattern, heat transfer and pressure drop in flow condensation; Part I: Pure and azeotropic refrigerants, Int. J. HVAC&R Res. 6 (2) (2000) 175–195.
[11] A. Cavallini, G. Censi, D. Del Col, L. Doretti, G.A. Longo, L. Rossetto, In-tube condensation of halogenated refrigerants, ASHRAE Trans. 108 (2002) 146–161.
[12] J. El Hajal, J.R. Thome, A. Cavallini, Condensation in horizontal tubes, part 1: two-phase flow pattern map, Int. J. Heat Mass Transfer 46 (18) (2003) 3349–3363.
[13] J.G. Collier, J.R. Thome, Convective Boiling and Condensation, Clarendon Press, Oxford, 1994.
[14] D. Steiner, Heat transfer to boiling saturated liquids, in: Verein Deutscher Ingenieure (Ed.), VDI-Warmeatlas (VDI Heat Atlas), VDI-Gesellschaft Verfahrenstechnik und Chemieingenieurswesen (GCV), Düsseldorf, 1993.
[15] Y. Taitel, A.E. Dukler, A model for predicting flow regime transitions in horizontal and near-horizontal gas–liquid flow, Am. Inst. Chem. Eng. (AIChE) J. 22 (1) (1976) 47–55.
[16] S.Z. Rouhani, E. Axelsson, Calculation of volume void fraction in the subcooled and quality region, Int. J. Heat Mass Transfer 13 (2) (1970) 383–393.
[17] O. Zürcher, J.R. Thome, D. Favrat, Evaporation of ammonia in a smooth horizontal tube: heat transfer measurements and predictions, J. Heat Transfer 121 (1) (1999) 89–101.
[18] J.R. Thome, J. El Hajal, A. Cavallini, Condensation in horizontal tubes, part 2: new heat transfer model based on flow regimes, Int. J. Heat Mass Transfer 46 (18) (2003) 3365–3387.
[19] J.R. Thome, Update on advances in flow pattern based two-phase heat transfer models, Exp. Therm. Fluid Sci. 29 (3) (2005) 341–349.
[20] A. Cavallini, D.D. Col, L. Doretti, M. Matkovic, L. Rosetto, C. Zilio, Condensation in horizontal smooth tubes: a new heat transfer model for heat exchanger design, Heat Transfer Eng. 27 (8) (2006) 31–38.
[21] K. Cho, S.J. Tae, Condensation heat transfer for R-22 and R-407C refrigerant–oil mixtures in a microfin tube with a U-bend, Int. J. Heat Mass Transfer 44 (11) (2001) 2043–2051.
[22] ASHRAE, ASHRAE Standard 41.4: method for measurement of proportion of lubricant in liquid refrigerant, American Society for Heating, Refrigeration, and Air-conditioning Engineers, 2006.
[23] S.J. Kline, F.A. McCintock, Describing uncertainties in single-sample experiments, Mech. Eng. 75 (1953) 3–8.
[24] REFPROP, NIST thermodynamic properties of refrigerants and refrigerant mixtures (REFPROP), Version 8.0, NIST Standard Reference Database 23, National Institute of Standards and Technology, Gaithersburg, MD, 2005.
[25] XProps, Thermal Analysis Partners, University of Maryland, MD, 2006. Available from: <http://www.thermalanalysispartners.com>.
[26] J.A. Olivier, L. Liebenberg, J.R. Thome, J.P. Meyer, Heat transfer, pressure drop, and flow pattern recognition during condensation inside smooth, helical micro-fin and herringbone tubes, Int. J. Refrig. 30 (4) (2007) 609–623.
[27] D.W. Shao, E. Granryd, Heat transfer and pressure drop of R-134a–oil mixtures in a horizontal condensing tube, Int. J. Refrig. 18 (8) (1995) 524–533.
[28] L.M. Schlager, M.B. Pate, A.E. Bergles, Evaporation and condensation of refrigerant–oil mixtures in a smooth tube and micro-fin tube, ASHRAE Trans. 94 (1988) 149–166.
[29] B. Sur, N.Z. Azer, Effect of oil on heat transfer and pressure drop during condensation of refrigerant-113 inside smooth and internally finned tubes, ASHRAE Trans. 97 (1991) 365–373.
[30] S.J. Eckels, M.B. Pate, In-tube evaporation and condensation of refrigerant–lubricant mixtures of HFC134a and CFC12, ASHRAE Trans. 97 (1991) 62–70.
[31] A. Cavallini, D. Del Col, G.A. Longo, L. Rossetto, Experimental investigation on condensation heat transfer and pressure drop of new HFC refrigerants (R134a, R125, R32, R410A, R236ea) in a horizontal tube, Int. J. Refrig. 24 (1) (2001) 73–87.
[32] W. Nusselt, Die oberachenkondensation des wasserdampfes, Z. Ver. Dt. Ing. 60 (1916) 541–546. 569–575.
[33] A. Cavallini, G. Censi, D. Del Col, L. Doretti, G.A. Longo, L. Rossetto, C. Zilio, Condensation inside and outside smooth and enhanced tubes – a review of recent research, Int. J. Refrig. 26 (4) (2003) 373–392.

Please cite this article in press as: R. Suliman et al., Improved flow pattern map for accurate prediction of the heat transfer coefficients during condensation of R-134a in smooth horizontal tubes and within the low-mass flux range, Int. J. Heat Mass Transfer (2009), doi:10.1016/j.ijheatmasstransfer.2009.08.017